Available online at www.sciencedirect.com
SCIENCE DIRECT
Catalysis Today 110 (2005) 98–107
CATALYSIS TODAY
www.elsevier.com/locate/cattod

Temperature profiles and residence time effects during catalytic partial oxidation and oxidative steam reforming of propane in metallic microchannel reactors

Ingrid Aartun [a,1], Hilde J. Venvik [a,*], Anders Holmen [a], Peter Pfeifer [b], Oliver Görke [b], Klaus Schubert [b]

[a] *Department of Chemical Engineering, Norwegian University of Science and Technology (NTNU), NO-7491 Trondheim, Norway*

[b] *Institute for Micro Process Engineering, Forschungszentrum Karlsruhe GmbH (FZK), Postfach 3640, DE-76021 Karlsruhe, Germany*

Available online 13 October 2005

Abstract

Microchanneled reactors made from Fecralloy and impregnated with Rh were studied in partial oxidation (POX) and oxidative steam reforming (OSR) reactions for production of hydrogen or synthesis gas. Temperature profiles obtained along the reactor axis confirmed that the metallic microchannel reactor is able to minimize temperature gradients and pointed to gas phase ignition in front of the reactor as the main reason for reduced syngas production and increased hydrocarbon by-product formation at the highest furnace temperatures. Addition of steam to the reactant mixture (OSR) resulted in increased formation of hydrogen relative to propane converted ($S^*(H_2)$), mainly in accordance with the water–gas shift reaction. Reducing the residence time below 10 ms at 800 °C gave increased $S^*(H_2)$ and CO selectivity and reduced by-product formation, indicating suppression of the gas phase reactions and possibly also direct formation of H_2 and CO as part of the reaction scheme. The Rh/Al_2O_3/Fecralloy microchannel reactor also shows good stability during more than 70 experiments of both POX and OSR with temperature cycling from 300 to 1000 °C.

Keywords: Hydrogen production; Partial oxidation; Steam reforming; Microchannel reactor; Temperature profiles; Rh; Fecralloy

1. Introduction

For the production of hydrogen or synthesis gas via fast reactions, i.e. oxidation reactions, high throughput reactor systems have long been considered promising for technological improvements. Increased throughput has been prospected for many chemical reactions by the use of so-called short contact time reactors. These are structured catalyst supports characterised by low pressure drop even with very high gas velocities, usually gauzes, monoliths or relatively open foam structures. Their application as car exhaust catalysts has led to the use of thermally and mechanically stable materials such as mixed oxides (ceramics) and high temperature alloys. Short contact time systems have over the last years received much attention as possible syngas/hydrogen generation systems [1–8]. They have also been studied for a number of other reactions such as dehydrogenation [9–16], and Fischer–Tropsch synthesis [17,18].

The conventional route from hydrocarbons to syngas is via steam reforming (SR), where the kinetics, and hence the throughput, to a large extent is limited by the rate at which the heat generated in external burners can be transferred to the catalytic bed where the endothermal reforming takes place [19]. Industrially, the heat generation has been transferred inside the reactor by autothermal reforming (ATR) and non-catalytic partial oxidation (POX). These concepts do, however, include homogeneous partial or complete oxidation zones at elevated temperature, which introduce challenges in terms of materials and formation of soot. The latter is particularly the case for POX, since oxygen to carbon ratios are low and the temperature rises to typically 1200–1500 °C [20]. In industrial ATR, oxygen and steam is co-fed, and homogeneous combustion is followed

* Corresponding author.
E-mail address: venvik@chemeng.ntnu.no (H.J. Venvik).
[1] Present address: Statoil R&D Centre, NO-7005 Trondheim, Norway.

0920-5861/$ – see front matter © 2005 Elsevier B.V. All rights reserved.
doi:10.1016/j.cattod.2005.09.001

by a fixed catalyst bed for equilibration of the gas [21]. This restricts the temperature and soot formation relative to POX, and has successfully been implemented in large syngas plants over the last years [22]. Less oxygen is also needed, the efficiency improves and the product H_2 to CO ratio is increased. The temperature gradients are, however, still large, and the transfer of heat from exothermic to endothermic reaction zones is facilitated mainly by convection.

Reduced temperatures at high throughput could be obtained through catalytic partial oxidation. Limited heat transport and fast exothermal reactions still make it difficult to control the syngas selectivity and temperature increase in (parts of) the POX catalyst [23]. Given sufficient contact time, partial and complete oxidation reactions are followed by water gas shift (WGS) and endothermal reforming reactions further down the catalyst bed, and the product gas composition is determined by thermodynamic equilibrium at the exit. It is thus of importance that the heat generated at the entrance of the catalyst is efficiently transported downstream.

Stoichiometric POX involves generation of more heat than necessary to drive the reaction. By replacing some of the oxygen with steam, heat generation and consumption could be more balanced. Co-feeding steam and oxygen and letting the exothermic oxidation reactions and endothermic reforming reactions proceed in close contact over the same catalyst may be referred to as oxidative or oxygen-assisted steam reforming (OSR), or oxy-steam reforming. This allows the distinction from the scheme associated with industrial ATR, with well separated homogeneous and catalytic zones and no external heating. The OSR scheme requires efficient heat transport along the reactor and a catalyst that is active and stable in both POX and SR. Based on thermodynamics, the addition of steam as a reactant should facilitate higher hydrogen production through WGS and steam reforming. However, as the contact time becomes shorter, the kinetics will determine to which extent the added steam will influence the product composition.

When the temperature increases, homogeneous reactions start to compete with the catalytic reactions. For propane, the onset of dehydrogenation and cracking reactions interferes with the regime of high conversion and syngas selectivity. The onset of gas phase reactions is connected to the catalysts ability to supply heat to the homogeneous reactions. A high extent of total oxidation reactions on the catalyst leads to high heat generation rates and high temperature. While the transfer of heat to the gas phase could be limited by e.g. radiation shielding by placing a solid structure directly in front and after the catalyst [24], a catalyst support with good heat transport properties could suppress the large local temperature maximum usually associated with the oxygen conversion zone of catalytic partial oxidation.

The reaction mechanisms of alkane catalytic partial oxidation have been much studied and debated in the literature [5,25–31]. It has been found that over some catalysts and under some conditions, H_2 and CO form as direct products from methane as well as ethane and propane, and not exclusively via downstream steam and/or dry reforming of the total oxidation products H_2O and CO_2. This could potentially facilitate extremely short contact times and thus very high throughput. However, the active catalysts are also active for consecutive oxidation of the syngas, and hence the oxygen concentration on the catalyst surface has to be sufficiently low.

Pt has been found to facilitate direct formation of both partial and total oxidation products, but H_2 and CO are readily oxidized as long as the oxygen conversion is incomplete. Pt is not found, however, to facilitate reactions with steam or CO_2, i.e. reforming and water–gas shift [5]. Rh has been shown to be more active for alkane conversion and more selective to syngas formation than alternative catalysts, i.e. Pt, Pd, Ir and Ni [5,32–34]. Both direct syngas formation and secondary reactions are facilitated by Rh, depending on the contact time [5]. The WGS reaction also proceeds over Rh at relatively short contact time in the relevant temperature regime [1,10,35,36].

Metallic microchannel reactors may offer solutions to some of the challenges described above. These systems have recently received attention as promising for several reactions relevant to hydrogen and syngas production, e.g. steam reforming [37–41], partial oxidation [42,43], oxidative steam reforming [43,44], water gas shift [45–47] and preferential oxidation of CO [48–50]. The high heat and mass transfer rates associated with such systems could lead to higher efficiencies, as conventional syngas production systems often are heat or mass transfer limited. The metallic structure also facilitates high axial heat transfer, which could suppress the formation of local temperature maxima, and thereby deactivation of the catalyst. The small reaction volumes offer an intrinsic safety, as high surface-to-volume ratios lead to radical quenching and thus avoidance of gas phase reactions. This allows for safe handling of otherwise explosive gas mixtures [51,52].

Stability is of particular importance since catalysts containing active metals on supports are not easily stabilised at these temperatures, and especially under exposure to oxygen and steam. Our and other studies indicate that Rh on particulate or structured supports is prone to sintering, and possibly also loss of active material, at high temperature [24,53]. Moreover, these effects are accelerated upon temperature cycling and increased steam concentration.

The scope of our work is to establish whether metallic microchannel reactors have special advantages in catalytic POX and OSR with respect to activity, product composition, temperatures and stability. In this paper, we particularly emphasize the temperature profiles taken along the reactor axis along with effects of varying the total gas flow, i.e. the residence time of the reactant mixture inside the catalyst.

2. Experimental

The metallic microchannel reactors were manufactured from Fecralloy (72.6% Fe, 22% Cr, 4.8% Al) at the Institute for Micro Process Engineering (IMVT) at Forschungszentrum Karlsruhe [54]. Three microchannel reactors of identical outer dimensions (length 20 mm, cross section 5.5 mm × 5.6 mm) were applied, and their physical data are given in Table 1. While reactor 1 and 2 are regular monolithic structures, reactor 3 was equipped with a 600 μm × 600 μm channel along the central

Table 1
Physical data of the microchannel reactors

	Reactor no.		
	1	2	3
Material	Fecralloy	Fecralloy	Fecralloy
H (mm) × W (mm) × L (mm)	5.5 × 5.6 × 20	5.5 × 5.6 × 20	5.5 × 5.6 × 20
No. of channels	676	676	572
Channel dimension (μm × μm)	120 × 130	100 × 120	100 × 120
Thermocouple channel dimension (μm × μm)	–	–	600 × 600
Geom. surface of channels (cm^2)	67.5	59.5	50.8
Porosity	0.34	0.26	0.22
Flow at 12.7 ms residence time (N ml/min)	1000	769	614
Impregnated with	Rh	–	–/Rh

axis to allow for temperature measurements inside the microchannel reactor. A photograph and a SEM-image of reactor 2 are given in Fig. 1. The reactors were oxidized in air at 1000 °C to form a thin alumina surface layer. Reactors 1 and 3 were impregnated with Rh as described below. Reactor 2 was used for reference experiments without the catalytic material, and experiments were conducted over reactor 3 both before and after impregnation in order to determine the effect of the catalytic material with respect to temperature. The catalytic effect of Rh on conversion and selectivity to main products has been reported previously [43]. Thus, results obtained using reactor 2 will only be briefly commented upon.

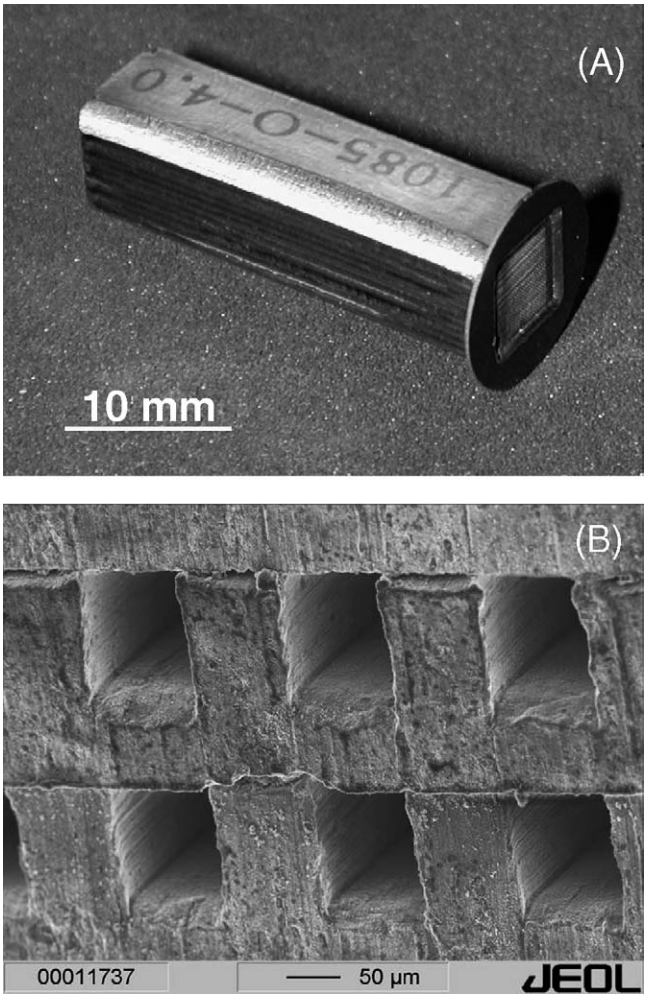

Fig. 1. (A) Photograph of reactor 2. (B) SEM-image of the channel openings of reactor 2.

The impregnation of reactors 1 and 3 was accomplished by passing an aqueous solution of $RhCl_3$ through the channels, including the 600 μm channel of reactor 3, followed by drying at 120 °C overnight. The mass increase resulting from impregnation corresponds to 1 and 0.9 mg Rh for reactors 1 and 3, respectively. The Rh/Al_2O_3/Fecralloy reactors were reduced in situ at 800 °C for 3 h in 10% H_2 in N_2 [43]. During experiments with changing C/O ratio in the feed (unpublished), coking was observed. The coke was burned off in air at 700 °C before the catalyst was reduced again, as described above.

The reaction experiments reported here were mainly performed at SINTEF/NTNU, Trondheim, but in reporting long term stability, data obtained at IMVT, Karlsruhe are also used. The two experimental set-ups consist of notably different reactor housings, temperature measurement arrangements, steam feed systems and analysis equipment, and have previously been described in more detail [8,42,43]. All conversion and selectivity data, as well as temperature and residence time effects are reported using a set-up were the microchannel reactors were contained in a quartz reactor inserted into a gold insulated furnace that allows visual inspection at elevated temperatures. 1 mm K-type thermocouples were placed inside thin quartz tubes to eliminate contributions from the small catalytic activity of the thermocouples themselves, one directly in front and one directly after reactors 1 and 2. For reactor 3, the thermocouple in front was replaced with a moveable 0.5 mm N-type thermocouple (without the quartz tube) to allow for measurements inside the 600 μm channel. Water was removed from the product stream by condensation and dry samples were analyzed by gas chromatography (Agilent G2891A MicroGC).

The experiments were carried out using a continuous reactant flow at near-to atmospheric pressure and furnace temperatures from 300 to 950 °C. The concentration of propane was kept the same for both POX and OSR. The reactant mixture consisted of propane, oxygen and nitrogen for POX, with a C/O ratio equal to 0.8 and N/O as for air. In case of OSR, steam was added to the feed and the C/O and H_2O/O_2 ratios were 0.5 and 2.0, respectively. The C/O and H_2O/O_2 ratios were chosen as optimum for POX and OSR according to reported values and previous experience [8,9,43]. Temperature dependent data were obtained using a total flow rate of 1000 N ml/min (0 °C, 101.3 kPa). Residence time effects were studied in a flow range of 400–2000 N ml/min. The water content in the product stream was estimated from the H- and O-balances, using N_2 as an internal standard to calculate the total volumetric flow after reaction.

A modified hydrogen selectivity (or productivity) was calculated according to Eq. (1):

$$S^*(H_2) = \frac{F_{tot,out}}{F_{tot,in}} \frac{C_{H_2,out}}{4C_{C_3H_8,in}X_{C_3H_8}} \quad (1)$$

where $F_{tot,in}$ and $F_{tot,out}$ are the total volumetric gas flows (N ml/min) at reactor inlet and outlet, respectively, $C_{H_2,out}$ the concentration of hydrogen in the outlet gas, $C_{C_3H_8,in}$ the concentration of propane in the feed gas and $X_{C_3H_8}$ the conversion of propane. $S^*(H_2)$ (1) expresses how much hydrogen is formed relative to propane converted, irrespective of steam content in the reaction mixture. It may thus exceed 1 for OSR experiments, whereas it is identical to a standard hydrogen selectivity for POX experiments. The residence time was calculated as the ratio of void volume inside the microchannel reactors to $F_{tot,in}$ [8,43].

The stability of the catalyst is evaluated using a range of data obtained over four test periods in the two different set-ups with a time span of approximately three years. During this period, minor changes in experimental procedure have been implemented related to refined GC-methods and calibration. The experiments for parameter variation are thus reported using the most recent procedure, whereas the whole dataset has been applied to verify the long term stability.

3. Results and discussion

3.1. Temperature profiles

Temperature profiles obtained along the reactor central axis of microchannel reactor 3 before and after impregnation with ~0.9 mg Rh are given in Fig. 2. The total reactant flow is 614 N ml/min to ensure the same residence time (12.7 ms) as for 1000 N ml/min in reactor 1 (see Table 1). Up to 700 °C furnace temperature, temperature gradients along the Al_2O_3/Fecalloy reactor are not present and furnace and reactor temperatures are virtually identical. Then there is a significant temperature peak (900 °C maximum) in front of the reactor at 750 °C furnace temperature during POX, indicating ignition of the gas phase. At the highest furnace temperature (800 °C), the maximum temperature appears well in front of the reactor (40–60 mm), and the flame could also be observed visually. This gas phase ignition is observed also during OSR. However, the smaller peaks in the temperature profile at 700 °C furnace temperature for OSR indicate that the transition is about to occur at this temperature. After gas phase ignition there are no temperature gradients over the Al_2O_3/Fecalloy reactor.

After impregnation with Rh, the reactor ignites between 400 and 500 °C during both POX and OSR. The catalytic ignition is accompanied by a temperature increase of around 50 °C. The catalyst temperature increase is relatively small compared to what may be expected using oxide-based structured catalysts such as ceramic monoliths or foams [8,24], or fixed particle beds [23,55], where peaks of several hundred K are usually observed. This is indicative of more efficient heat transport in the metallic microchannel reactors, resulting in a suppression of local temperature build-up and the associated increased conversion [56]. Radial temperature gradients may also be present when significant gradients exist in the axial direction, but these would be extremely difficult to measure and are expected to be small.

When the furnace temperature is increased above ~700 °C, the gas phase in front of the Rh/Al_2O_3/Fecralloy reactor ignites during both POX and OSR. Upon further heating, the temperature inside the microchannel reactor is almost identical to the furnace temperature. The bulk of the oxygen is converted in homogenous oxidation reactions in the gas phase, but WGS and steam reforming can still proceed on the catalyst provided the residence time is long enough. A reaction scheme similar to conventional ATR is thus feasible. Besides furnace temperature, gas phase ignition could be dependent on some other factors: First, the presence of dead volumes where turbulence and backmixing may take place, and where the linear gas flow is substantially lower than in the microchannels. If the gas velocity is higher than the flame velocity, ignition of the gas phase can be avoided [57]. Second, the temperature of the part of the catalyst exposed to the gas volume at the front of the microchannel reactor is an important factor, and may be influenced by the activity and loading of the catalyst as well as the heat conductivity of the catalytic system. This was observed in previous studies of Rh-impregnated foams [56,58], and explains why the gas phase ignition occurs at lower furnace temperature for Rh/Al_2O_3/Fecralloy as compared to Al_2O_3/Fecralloy.

3.2. Conversion and selectivity

The conversion of reactants, $S^*(H_2)$ and the selectivity to all carbon-containing products as a function of the furnace temperature during POX and OSR in reactor 1 are reported in Fig. 3. The conversion of propane and oxygen is steadily increasing over the furnace temperature range 500–800 °C, until almost complete conversion is reached around 800 °C. Complete conversion of propane is reached at 800 and 850 °C furnace temperature for POX and OSR, respectively. While complete conversion of oxygen is reached for POX at 900 °C, trace amounts of oxygen are still detected at 950 °C for OSR.

$S^*(H_2)$ and the CO selectivity both display a maximum at a furnace temperature of 750 °C during POX and 700 °C during OSR. These maxima are followed by a sharp decrease from 750 to 800 and 700 to 750 °C, for POX and OSR respectively, and then a gradual increase with temperature. We interpret the sharp decrease in syngas formation to be a result of gas phase ignition in front of the catalyst. The gas phase ignition at lower furnace temperature for OSR as compared to POX is not easily explained, since the total amount of oxygen converted and thus the catalyst temperature are the highest during POX. A possible explanation could be the improved heat conductivity in the gas phase when some of the air in the feed gas is replaced with steam. Gas phase ignition temperatures of 800 °C (POX) and 750 °C (OSR) are only partly in agreement in with the temperature profiles of Fig. 2C and D, which indicate gas phase ignition at approximately 50 °C lower temperature for both reactions. This discrepancy may, however, originate from the

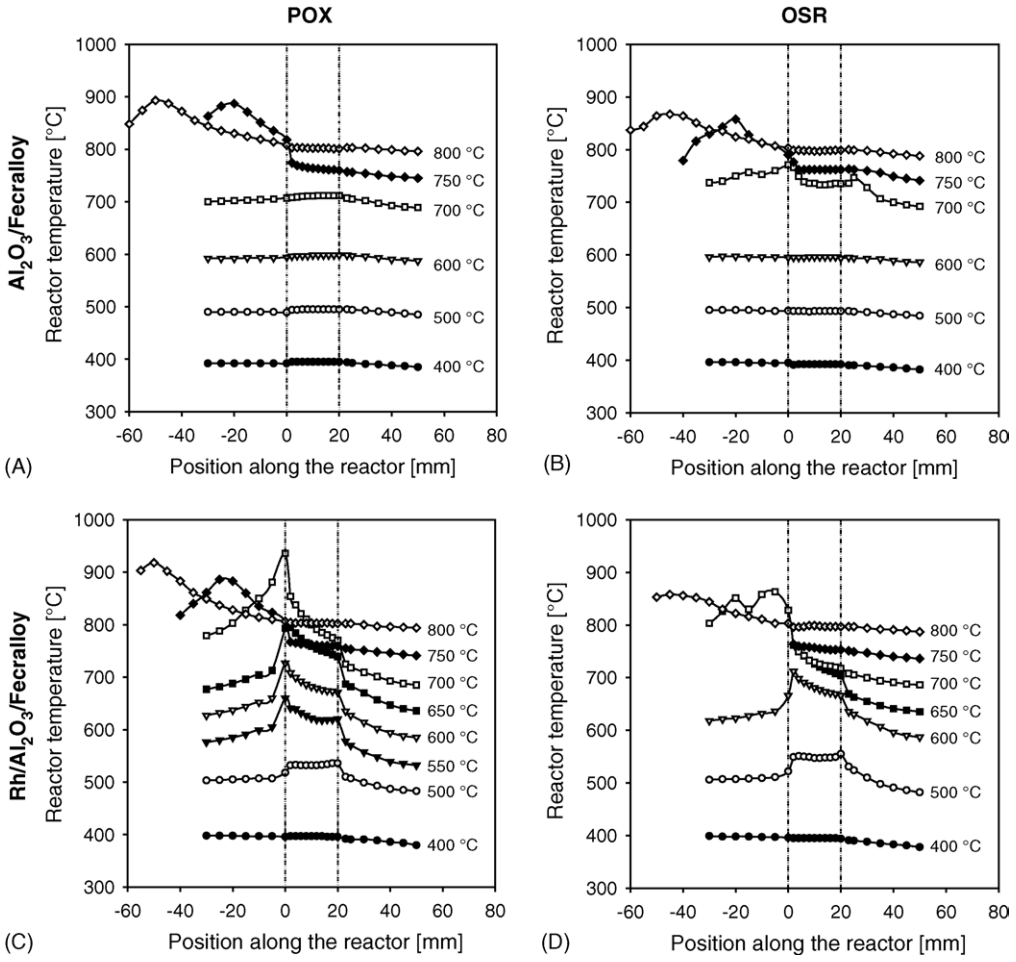

Fig. 2. Temperature profiles in Al_2O_3/Fecalloy (A and B) and Rh/Al_2O_3/Fecralloy (C and D) for both POX (A and C) and OSR (B and D). The vertical lines represent the start and end of the reactor.

difference in linear gas velocity in the dead volume in front of the two microchannel reactors, as the total flow is 1000 and 614 N ml/min in reactors 1 and 3, respectively. The gas phase ignition seems to occur at a lower furnace temperature when the total flow is lowered. In addition, homogeneous reactions taking place in the larger channel of reactor 3, as observed visually, may influence the temperature measurement.

S*(H_2) is significantly higher during OSR as compared to POX as long as gas phase ignition does not occur (below 700–750 °C). The addition of steam also reduces the selectivity to CO and increases the selectivity to CO_2. WGS thus seems to be the main route to the increase in S*(H_2) when steam is added to the feed, but contributions from dry and steam reforming cannot be excluded. This is in accordance with other studies showing that WGS proceeds over Rh and Pt catalysts at higher rates than steam reforming at temperatures above 600 °C [35,36]. After gas phase ignition, the main effect of changing POX with OSR conditions appears to be reduced formation of CO without increased hydrogen formation. This is related to the higher formation of hydrocarbon by-products when oxygen concentration is reduced and steam is added to the reactant mixture.

Hydrocarbon by-products include methane, ethane, ethene, ethyne, propene and trace amount of C_{4+} compounds. These are observed in varying amounts depending on temperature, as can be seen from Fig. 3C and D for POX and OSR, respectively. The propene selectivity has a maximum value (∼3%) around 700 °C for POX and 750 °C for OSR. A significant increase in the formation of methane and ethene occurs from 750 to 800 and 700 to 800 °C, for POX and OSR respectively, coinciding with ignition of the gas phase. Methane and ethene also show increased selectivity upon addition of steam, and they both undergo maxima and then decrease upon further temperature increase. The observed variations in propene, ethene and methane selectivities are consistent with a product distribution as for dehydrogenation and homogeneous cracking. Steam is often added to suppress carbon formation during cracking, but is not considered to be a part of the homogeneous reaction scheme [59]. The increased formation of hydrocarbons under OSR conditions thus reflects the lower concentration of oxygen fed, which again results in a smaller part of the propane being converted in oxidation reactions. The ethane C-selectivity should be twice that of methane according to the cracking scheme, but we observe considerable higher methane than ethene selectivity. Both compounds may be converted in different downstream catalytic reactions, for which ethene is generally more active than methane. Methane may also be formed from other reactions.

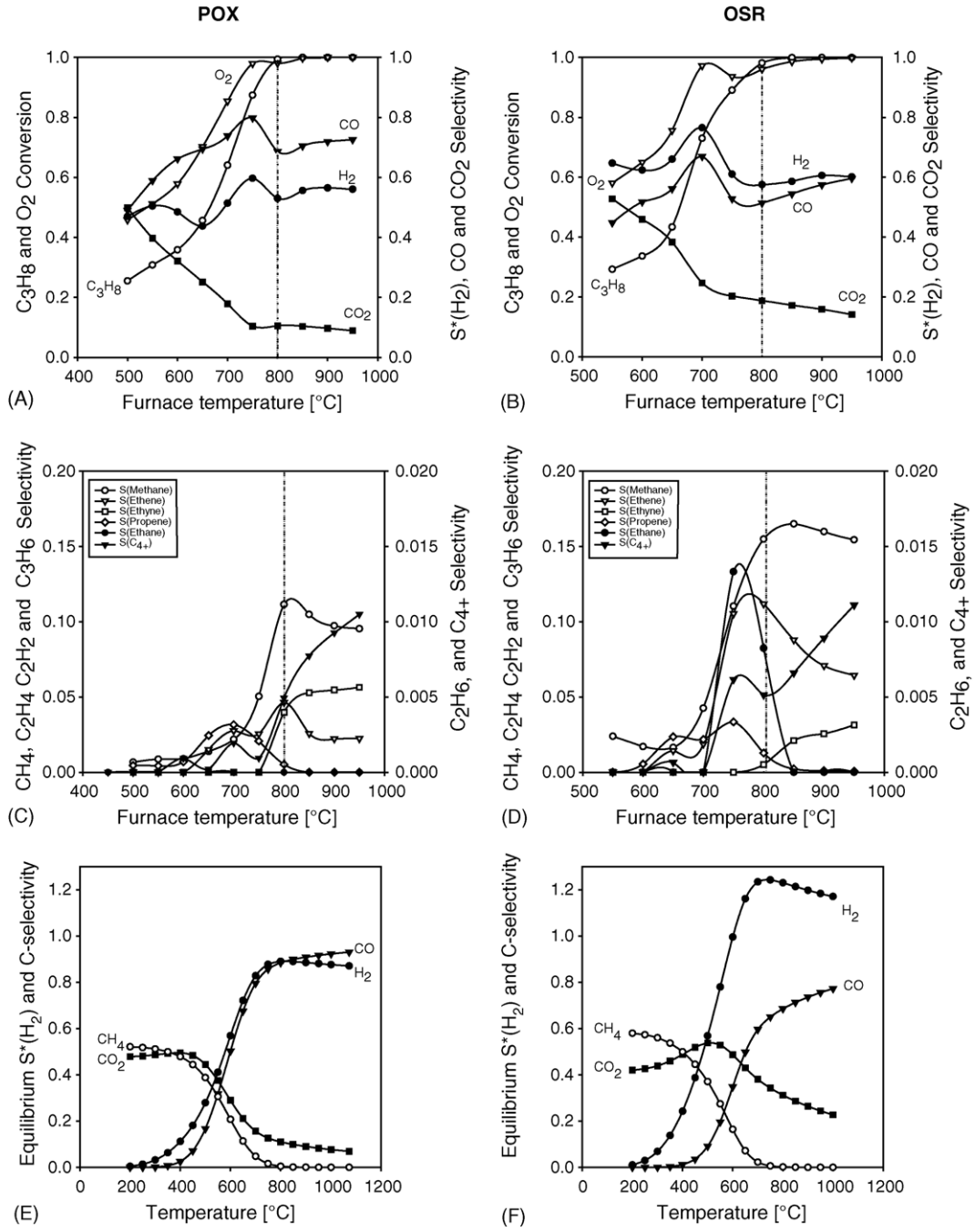

Fig. 3. Conversion, S*(H_2) and main carbon product selectivity (A and B) and by-product selectivity (C and D) as a function of furnace temperature for partial oxidation (A and C) and oxidative steam reforming (B and D). The feed gas flow was 1000 N ml/min, leading to a residence time of 12.7 ms. The vertical lines represent the temperature used in the residence time effect experiments. The equilibrium S*(H_2) and main carbon product selectivity predicted by minimisation of Gibb's free energy (HYSYS) using the experimental POX and OSR reactant compositions are also shown (E and F).

Ethyne formation generally sets on with gas phase ignition and increases with temperature, and is slightly more abundant during POX. This shows that ethyne is formed homogeneously as a function of the maximum temperature in the system only. Ethane and C_{4+} compounds are detected in much lower concentrations. During POX, a small peak (<0.2%) in ethane formation is found at 600 °C, and no ethane is found above 700 °C. The highest ethane selectivity during OSR coincides with gas phase ignition at 750 °C and the maximum (~1.3%) is notably higher than for POX. The formation of ethane is in accordance with hydrogenolysis of propane. The C_{4+} selectivity sees some small variations at the lower temperatures, but increases substantially with gas phase ignition and further increasing furnace temperatures.

Also previous work, reporting experiments over un-impregnated microchannel reactors [43] and alumina foams [8], lead to the conclusion that hydrocarbon by-products are mainly formed homogeneously, and particularly when gas phase ignition occurs in front of the structured support. The total selectivity to by-products was also significantly higher

with the microchannel Rh/Al_2O_3/Fecralloy reactor compared to Rh-impregnated alumina foams of comparable loadings. This appears, however, to be more related to the total reactor configuration and whether gas phase ignition apart from the catalyst is facilitated, and we expect very little of the hydrocarbons to actually form in the microchannels. By minimizing the dead volume in front of the microchannel reactor, the syngas formation could possibly be increased.

Comparable equilibrium main carbon product selectivity and $S^*(H_2)$ as calculated by minimization of Gibb's free energy using the HYSYS software are shown in Fig. 3E and F. The calculation predicts complete conversion of propane and oxygen at all temperatures. Comparing equilibrium calculations to the data obtained has certain limitations because it is difficult to determine which measured temperature gives the most relevant comparison. Furthermore, thermodynamic equilibrium does not predict formation of the C_{2+} by-products found in significant amounts. The equilibrium $S^*(H_2)$ value reaches maximum values of 0.89 and 1.24 around 800 °C for POX and OSR, respectively. Increasing the temperature further leads to an almost constant syngas ($H_2 + CO$) production, but the H_2/CO-ratio decreases slightly due to reverse water gas shift. When the gas phase has not ignited, the outlet temperature measured is approximately 100 °C higher than the furnace temperature. Comparing the products obtained (Fig. 3A and B) for the outlet temperature measured to corresponding equilibrium values shows that $S^*(H_2)$ and the CO selectivity lies well below equilibrium, particularly at the highest temperatures. $S^*(H_2)$ deviates more than the CO selectivity, which could indicate that hydrogen is more readily combusted than CO. The methane selectivity increases with increasing temperature, opposite of the equilibrium prediction.

3.3. Residence time effects

Fig. 4 shows the variation in conversion, $S^*(H_2)$ and carbon product selectivity as a function of residence time for both POX and OSR reactions in reactor 1. The changes in the flow rate were made at a furnace temperature of 800 °C in order to compare the product composition when nearly complete conversion of propane is reached for a total flow of 1000 N ml/min. The catalyst temperatures should be higher at low residence time due to more heat produced in the exothermic reactions, provided that the conversion is upheld. The measured outlet temperature increases approximately 50 °C from the longest to the shortest residence time. Since the data were obtained using reactor 1, a corresponding increase in the catalyst maximum temperature has not been verified.

There is a noticeable increase in $S^*(H_2)$ and the CO selectivity for residence times below 10 ms for both POX and OSR. This is, however, accompanied by a decrease in oxygen and propane conversion. The $S^*(H_2)$ and CO selectivity increase at very short residence times may partly be explained by increased catalyst temperatures, but may also indicate that the direct formation of hydrogen and CO is part of the reaction scheme, as has also been reported by others [5,28,30,31,60]. The presence of a direct mechanism implies that ignition of the gas phase in front ot the microhannel reactor is suppressed at sufficiently high GHSV. The H_2/CO ratio should not, however, be influenced by the addition of steam to the reactant mixture if direct formation of syngas was the only route to syngas formation. Here, the H_2/CO ratio increases with decreasing residence time in OSR, whereas it decreases in POX. At the shortest contact time, $S^*(H_2)$ is 60.3 and 69.5% for POX and OSR, respectively, and the corresponding CO selectivity is 75.2 and 60.0%. This implies that WGS and parallel and consecutive reactions leading to deep oxidation is participating. The hydrogen yield is at its highest at 8.4 ms for both reactions. No major effects of changing flow were observed at residence times above 20 ms, except for a small increase in oxygen conversion with increasing residence time during OSR, and the syngas formation is still well below equilibrium.

Methane, ethene, ethyne and C_{4+} selectivities follow similar trends and generally decrease when the residence time is lowered below 10 ms, while the selectivities to propene and ethane increase below 10 ms. This supports the proposed suppression of gas phase ignition by high linear gas flows. The selectivity to ethyne undergoes a maximum during both POX and OSR at residence times between 12 and 20 ms, corresponding to flow rates of 500–1000 N ml/min. Temperature profiles obtained at different residence times could possibly verify our hypothesis on suppressed gas phase ignition and increased maximum catalyst temperatures at high flow rates.

3.4. Stability

Finally, in Table 2 we attempt to summarise more than 70 experiments over the microchannel Rh/Al_2O_3/Fecralloy reactor 1 with cycling of the reactor temperature from room temperature to ∼1000 °C, in order to indicate the promising stability of this system. The experiments have taken place over a period of 3 years in four test periods. We have in two different experimental set-ups mainly switched between the POX and OSR conditions as specified here and used in the table, but in addition some other pre-treatment and reactant mixtures (e.g. C/O variations) were applied. Table 2 compares $S^*(H_2)$ and CO selectivity data at the lowest temperature where complete conversion occurs, since this may represent the most comparable reactor temperatures. The first and last POX data measured in the same experimental set-up indicate that the catalyst has not deactivated.

The table reflects that the experimental set-ups are far from identical and not directly comparable. Experiments in Karlsruhe – reproducible in that set-up – need higher furnace temperatures (1000 °C) to reach complete conversion, but give the highest $S^*(H_2)$ and H_2/CO ratio at complete conversion. In comparison, a furnace temperature of only 900 °C is needed to obtain complete conversion in the Trondheim set-up, but with lower total syngas formation and H_2/CO ratio. The difference in temperature originates from the thermocouple regulating the furnace being very close to the microchannel reactor in the Karlruhe set-up, while in Trondheim, the thermocouple is placed several centimetres away from the reactor. The heat

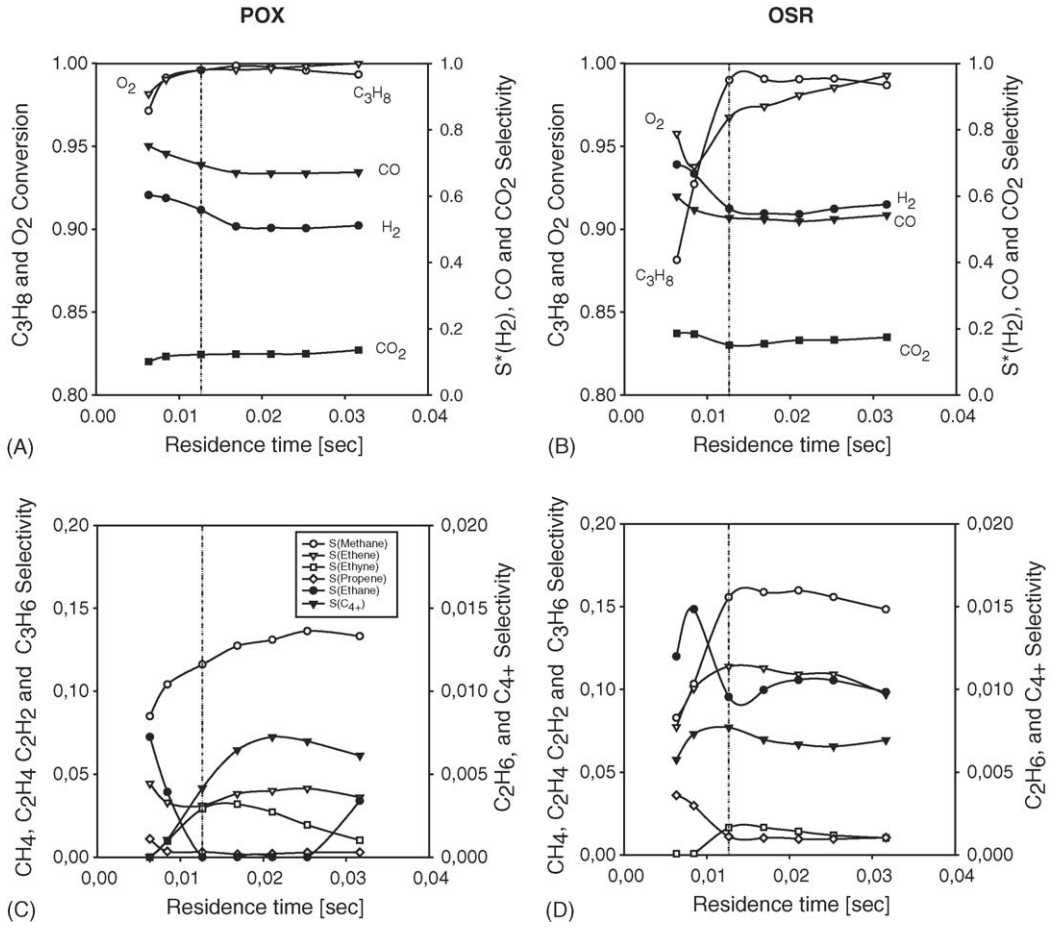

Fig. 4. Conversion, $S^*(H_2)$ and main carbon product selectivity (A and B) and by-product selectivity (C and D) for partial oxidation (A and C) and oxidative steam reforming (B and D) as a function of residence time. The furnace temperature was 800 °C. The vertical lines represent a feed gas flow of 1000 N ml/min, as used in the temperature effect experiments. Legend of C is also valid for D.

evolved during reaction will therefore influence the regulation of the heating coil in the Karlsruhe set-up. The higher $S^*(H_2)$ and slightly lower CO selectivity obtained in Karlsruhe could be explained by a more local heating of the microchannel reactor that leads to a lower temperature of the feed gas entering the microchannels and thereby prevention of gas phase ignition in front of the reactor. Moreover, the table as well as the total dataset indicate that the catalyst may have undergone some changes during test period 2 in Karlsruhe. This appears to be related to a few cycles of oxidation and reduction for coke removal after C/O variation as described in the experimental section. The treatment ''more than recovered'' the original activity, as can be seen from the improvement in the Karlsruhe POX data.

The reason behind the good stability remains to be found, and more systematic studies are in progress. The metallic

Table 2
$S^*(H_2)$ and CO selectivity (%) for POX and OSR at full conversion after repeated temperature cycling

	POX				OSR			
	$X(C_3H_8)$	$X(O_2)$	$S^*(H_2)$	$S(CO)$	$X(C_3H_8)$	$X(O_2)$	$S^*(H_2)$	$S(CO)$
Test period 1 Trondheim	100	100	49.0	76.1	–	–	–	–
Test period 2 Karlsruhe	100	100	50.5	59.0	–	–	–	–
Test period 3 Karlsruhe	100	100	68.0	69.0	100	100	81.5	57.0
Test period 4 Trondheim	100	100	59.7	73.3	100	99.7	62.7	60.4

More than 70 experimental cycles have been performed between the first and last measurements. Furnace temperatures were 900 °C for POX and 950 °C for OSR in the experiments conducted in Trondheim and 1000 °C for both reactions in experiments conducted in Karlsruhe.

structures ability to transport heat and thereby suppress local hot-spots on the surface could be beneficial, together with the ability to quench strongly exothermic oxidation reactions in the gas phase inside the narrow microchannels. Nevertheless, since the temperature is still high, the alumina layer created by oxidation of Fecralloy appears to stabilise the catalyst particles. The nature of the catalytic layer will be investigated by novel characterisation techniques to obtain a better understanding of the stability. Loss of Rh from the catalyst is very difficult to detect, and cannot be excluded for the microchannel Fecralloy reactors despite the unchanged activity.

4. Conclusions

Temperature profiles obtained along the reactor axis show that the metallic microchannel reactor is able to minimize temperature gradients due to exothermal reactions during partial oxidation and oxidative steam reforming of propane. At sufficiently high furnace temperature, the gas phase in front of the Rh/Al_2O_3/Fecralloy microchannel reactor ignites. Gas phase ignition leads to lower syngas formation and higher selectivity to total oxidation products and hydrocarbon by-products.

The modified hydrogen selectivity ($S^*(H_2)$) and the CO selectivity display a maximum at the highest furnace temperature without gas phase ignition. At this furnace temperature, 750 and 700 °C for POX and OSR, respectively, propane and oxygen conversion is incomplete. The hydrogen formation is increased in OSR as compared to POX, the main contribution being the water–gas shift reaction.

Variation of the total flow rate at constant furnace temperature results in decreased propane and oxygen conversion along with increased $S^*(H_2)$ and CO selectivity and reduced hydrocarbon by-product formation at residence times below 10 ms for both POX and OSR. This indicates that gas phase ignition is suppressed at sufficiently high GHSV.

The Rh/Al_2O_3/Fecralloy microchannel reactor also shows promising stability, since it has been found not to deactivate after more than 70 experiments at POX or OSR conditions with temperature cycling from 300 to 1000 °C. The reason behind the good stability should be investigated by characterisation. Stability, together with increased $S^*(H_2)$ and CO selectivity at short contact time and the apparent ability of the reactor to suppress gas phase reactions inside the microchannels indicate that the Rh/Al_2O_3/Fecralloy microchannel reactor should be studied for further optimisation as a hydrogen producing system.

Acknowledgement

This work has been supported by the Research Council of Norway and Statoil ASA through the Gas Technology Center NTNU-SINTEF.

References

[1] K. Heitnes Hofstad, B. Andersson, A. Holmgren, O.A. Rokstad, A. Holmen, Stud. Surf. Sci. Catal. 107 (1997) 415.
[2] A.S. Bodke, S.S. Bharadwaj, L.D. Schmidt, J. Catal. 179 (1998) 138.
[3] L.D. Schmidt, E.J. Klein, C.A. Leclerc, J.J. Krummenacher, K.N. West, Chem. Eng. Sci. 58 (2003) 1037.
[4] B.E. Traxel, K.L. Hohn, Appl. Catal. A 244 (2003) 129.
[5] A. Beretta, P. Forzatti, Chem. Eng. J. 99 (2004) 219.
[6] D. Neumann, G. Veser, AIChE J. 51 (2005) 210.
[7] K.A. Williams, C.A. Leclerc, L.D. Schmidt, AIChE J. 51 (2005) 247.
[8] B. Silberova, H.J. Venvik, A. Holmen, Catal. Today 99 (2005) 69.
[9] M. Huff, L.D. Schmidt, J. Catal. 149 (1994) 127.
[10] M. Huff, P.M. Torniainen, L.D. Schmidt, Catal. Today 21 (1994) 113.
[11] M. Fathi, R. Lodeng, E.S. Nilsen, B. Silberova, A. Holmen, Catal. Today 64 (2001) 113.
[12] A. Beretta, E. Ranzi, P. Forzatti, Chem. Eng. Sci. 56 (2001) 779.
[13] F. Donsi, R. Pirone, G. Russo, J. Catal. 209 (2002) 51.
[14] F. Donsi, R. Pirone, G. Russo, Catal. Today 91–92 (2004) 285.
[15] J.J. Krummenacher, L.D. Schmidt, J. Catal. 222 (2004) 429.
[16] B. Silberova, M. Fathi, A. Holmen, Appl. Catal. A 276 (2004) 17.
[17] A.-M. Hilmen, E. Bergene, O.A. Lindvag, D. Schanke, S. Eri, A. Holmen, Catal. Today 69 (2001) 227.
[18] R.M. de Deugd, F. Kapteijn, J.A. Moulijn, Catal. Today 79–80 (2003) 495.
[19] W. Balthasar, D.J. Hambleton, Int. J. Hydrogen Energy 5 (1980) 21.
[20] M.H. Eikani, Can. Pat. Appl. (2004).
[21] J.R. Rostrup-Nielsen, Catal. Today 18 (1993) 305.
[22] K. Aasberg-Petersen, J.-H. Bak Hansen, T.S. Christensen, I. Dybkjaer, P.S. Christensen, C. Stub Nielsen, S.E.L. Winter Madsen, J.R. Rostrup-Nielsen, Appl. Catal. A 221 (2001) 379.
[23] T. Ioannides, X.E. Verykios, Catal. Lett. 47 (1997) 183.
[24] H. Hickman, E.A. Haupfear, L.D. Schmidt, Catal. Lett. 17 (1993) 223.
[25] M. Prettre, C. Eichner, M. Perrin, T. Faraday Soc. 43 (1946) 335.
[26] D. Dissanayake, M.P. Rosynek, K.C.C. Kharas, J.H. Lunsford, J. Catal. 132 (1991) 117.
[27] R.H. Jones, A.T. Ashcroft, D. Waller, A.K. Cheetham, J.M. Thomas, Catal. Lett. 8 (1991) 169.
[28] V.R. Choudhary, A.S. Mamman, S.D. Sansare, Angew. Chem. Int. Ed. Engl. 31 (1992) 1189.
[29] E.P.J. Mallens, J.H.B.J. Hoebink, G.B. Marin, Catal. Lett. 33 (1995) 291.
[30] K. Heitnes Hofstad, T. Sperle, O.A. Rokstad, A. Holmen, Catal. Lett. 45 (1997) 97.
[31] W.Z. Weng, M.S. Chen, Q.G. Yan, T.H. Wu, Z.S. Chao, Y.Y. Liao, H.L. Wan, Catal. Today 63 (2000) 317.
[32] P.M. Torniainen, X. Chu, L.D. Schmidt, J. Catal. 146 (1994) 1.
[33] S.S. Bharadwaj, L.D. Schmidt, J. Catal. 146 (1994) 11.
[34] S. Ayabe, H. Omoto, T. Utaka, R. Kikuchi, K. Sasaki, Y. Teraoka, K. Eguchi, Appl. Catal. A 241 (2003) 261.
[35] D. Wolf, M. Barre-Chassonnery, M. Hohenberger, A. van Veen, M. Baerns, Catal. Today 40 (1998) 147.
[36] C. Wheeler, A. Jhalani, E.J. Klein, S. Tummala, L.D. Schmidt, J. Catal. 223 (2004) 191.
[37] P. Pfeifer, M. Fichtner, K. Schubert, M.A. Liauw, G. Emig, in: Proceedings of the Third International Conference on Microreaction Technology (IMRET 3), Frankfurt, April 18–21, 1999), p. 372.
[38] P. Pfeifer, K. Schubert, M.A. Liauw, G. Emig, Chem. Eng. Res. Des. 81 (2003) 711.
[39] G. Kolb, R. Zapf, V. Hessel, H. Lowe, Appl. Catal. A 277 (2004) 155.
[40] Y. Men, H. Gnaser, R. Zapf, V. Hessel, C. Ziegler, G. Kolb, Appl. Catal. A 277 (2004) 83.
[41] A.Y. Tonkovich, S. Perry, Y. Wang, D. Qiu, T. LaPlante, W.A. Rogers, Chem. Eng. Sci. 59 (2004) 4819.
[42] M. Fichtner, J. Mayer, D. Wolf, K. Schubert, Ind. Eng. Chem. Res. 40 (2001) 3475.
[43] I. Aartun, T. Gjervan, H. Venvik, O. Gorke, P. Pfeifer, M. Fathi, A. Holmen, K. Schubert, Chem. Eng. J. 101 (2004) 93.
[44] C. Horny, L. Kiwi-Minsker, A. Renken, Chem. Eng. J. 101 (2004) 3.
[45] A.Y. Tonkovich, J.L. Zilka, M.J. LaMont, Y. Wang, R.S. Wegeng, Chem. Eng. Sci. 54 (1999) 2947.

[46] Q. Ming, P. Irving, Proceedings of the 226th ACS National Meeting, Abstracts of Papers, New York, NY, USA, September 7–11, 2003.
[47] G. Kolb, R. Zapf, H. Pennemann, V. Hessel, H. Loewe, in: Proceedings of the AIChE Spring National Meeting, New Orleans, LA, USA, April 25–29, 2004), p. 19.
[48] L. Bednarova, H. Chen, X. Ouyang, Proceedings of the 226th ACS National Meeting, Abstracts of Papers, New York, NY, USA, September 7–11, 2003.
[49] G. Chen, Q. Yuan, H. Li, S. Li, Chem. Eng. J. 101 (2004) 101.
[50] X. Ouyang, R.S. Besser, J. Power Sour. 141 (2005) 39.
[51] M.T. Janicke, H. Kestenbaum, U. Hagendorf, F. Schuth, M. Fichtner, K. Schubert, J. Catal. 191 (2000) 282.
[52] G. Veser, Chem. Eng. Sci. 56 (2001) 1265.
[53] B. Silberova, H.J. Venvik, J. Walmsley, A. Holmen, Catal. Today 100 (2005) 457.
[54] K. Schubert, W. Bier, J. Brandner, M. Fichtner, C. Franz, G. Linder, in: Proceedings of the Second International Conference on Microreaction Technology (IMRET 2), New Orleans, March 8–12, 1998, Paper no. 9d.
[55] B. Li, K. Maruyama, M. Nurunnabi, K. Kunimori, K. Tomishige, Appl. Catal. A 275 (2004) 157.
[56] I. Aartun, B. Silberova, H.J. Venvik, P. Pfeifer, O. Görke, K. Schubert, A. Holmen, Catal. Today 105 (2005) 469.
[57] K. Heitnes Hofstad, J.H.B.J. Hoebink, A. Holmen, G.B. Marin, Catal. Today 40 (1998) 157.
[58] B. Silberova, I. Aartun, H.J. Venvik, J.C. Walmsley, A. Holmen, in preparation.
[59] R. Lødeng, O.A. Lindvag, S. Kvisle, H. Reier-Nielsen, A. Holmen, Appl. Catal. A 187 (1999) 25.
[60] L.D. Schmidt, M. Huff, Catal. Today 21 (1994) 443.